

Beyond Boundary Frames: Audio-Visual Semantic Guidance for Context-Aware Video Interpolation

Yuchen Deng^{1,2} Xiuyang Wu¹ Hai-Tao Zheng^{1,2} Jie Wang^{1,2} Feidiao Yang^{2,†} Yuxing Han^{1,†}

¹Shenzhen International Graduate School, Tsinghua University ²Pengcheng Laboratory

{dyc23, jie-wang24}@mails.tsinghua.edu.cn {zheng.haitao, yuxinghan}@sz.tsinghua.edu.cn
xiuyangwu23@gmail.com yangfd@pcl.ac.cn

Abstract

Handling fast, complex, and highly non-linear motion patterns has long posed challenges for video frame interpolation. Although recent diffusion-based approaches improve upon traditional optical-flow-based methods, they still struggle to cover diverse application scenarios and often fail to produce sharp, temporally consistent frames in fine-grained motion tasks such as audio-visual synchronized interpolation. To address these limitations, we introduce BBF (Beyond Boundary Frames), a context-aware video frame interpolation framework, which could be guided by audio/visual semantics. First, we enhance the input design of the interpolation model so that it can flexibly handle multiple conditional modalities, including text, audio, images, and video. Second, we propose a decoupled multimodal fusion mechanism that sequentially injects different conditional signals into a DiT backbone. Finally, to maintain the generation abilities of the foundation model, we adopt a progressive multi-stage training paradigm, where the start-end frame difference embedding is used to dynamically adjust both the data sampling and the loss weighting. Extensive experimental results demonstrate that BBF outperforms specialized state-of-the-art methods on both generic interpolation and audio-visual synchronized interpolation tasks, establishing a unified framework for video frame interpolation under coordinated multi-channel conditioning.

1. Introduction

Video frame interpolation (VFI) aims to synthesize intermediate frames given boundary frames. Currently, VFI has attracted growing attention from both academia and industry, supporting applications in film and animation production [45], generating motion videos [6, 23, 27], novel view synthesis [3, 12, 62] and social media content creation [11, 52, 55]. Nevertheless, whether conventional

optical-flow interpolation or emerging diffusion-based interpolation, existing methods address only a subset of needs and remain challenged by diverse real-world scenarios, especially those involving fast, non-linear, fine-grained motion across extended time spans.

Most conventional video frame interpolation methods [22, 28–30, 39, 44, 45, 56, 57] rely on estimating bidirectional optical flow between starting and ending frames to synthesize the intermediate frames. However, since predicting bilateral flow from two frames is an ill-posed problem with many possible solutions in essence [15], most of them can only produce an over-smoothed mean solution degrading spatial details and temporal sharpness.

Recent advances in diffusion models have achieved impressive visual fidelity in image synthesis, which has inspired researchers to explore their application to video frame interpolation [24, 25, 34, 51]. These diffusion-based approaches typically operate in a latent space to directly predict and decode intermediate-frame representations from the start and end frames, thereby avoiding explicit flow-based warping and offering a promising alternative to traditional methods. However, despite these advantages, diffusion-based methods still struggle with large and complex motions, primarily due to the difficulty of denoising in a high-dimensional latent space and the limited expressiveness of current diffusion backbones. Moreover, previous studies [61] have shown that conventional latent-space diffusion contributes little to improving the quality of interpolated frames. Accordingly, researchers have improved the diffusion-based interpolation model by adopting multiple methods, such as hierarchical diffusion models [15] and multi-scale feature fusion [61] based on Diffusion Transformer (DiT) [40], enabling the capture of fine-grained details across motion scales and yielding a more effective diffusion process.

Although these methods can perform interpolation between boundary frames over short temporal spans, they are insufficient to meet the needs of diverse scenarios, especially those involving fast, non-linear, fine-grained motions

over longer windows, such as audio-visual synchronized interpolation tasks. In such cases, existing methods are struggling to produce videos that are contextually semantically aligned and temporally consistent. These limitations primarily arise because existing interpolation models ignore auxiliary conditioning signals, which are frequently obtainable from the scene beyond the boundary frames. For example, when provided with a pair of contiguous frames, the model is expected to exploit contextual information from the preceding and subsequent content. Similarly, when we need to edit a high-intensity speech video, the audio corresponding to the target segment is available.

To address the limitations of existing VFI methods, especially under fast, non-linear, and long-range fine-grained motion, we optimized the interpolation input types of the frame interpolation model, which include: text, audio, images, and video. However, how to integrate multiple modal condition information and achieve diversified video generation remains challenging. To this end, we propose BBF, a context-aware video frame interpolation framework which could be guided by audio/visual semantics. Concretely, we adopt a video interpolation mask mechanism based on pixel-level constraints of boundary frames. During the training and inference process, the starting and ending frames are encoded into the primary query tokens by a 3D encoder and fixed to both ends along the time dimension respectively. By integrating the global self-attention mechanism, in each denoising step, each position can directly focus on the starting and ending latency. Meanwhile, to achieve multimodal fusion more effectively, we propose a decoupled cross-modal fusion mechanism, which injects three different modal information: text, audio, and images, into the DiT backbone in sequence through cross-attention. Finally, to prevent any single modality from dominating generation, we employ a staged paradigm schedule that first enforces boundary-frame consistency constraints and then progressively increases audio conditioning, along with dynamic loss reweighting over the course of training. This combination effectively balances global structure and fine details in the synthesized videos.

Extensive experiments are conducted to evaluate our proposed method, which demonstrates notable superiority over existing competitors. Specifically, on generic interpolation benchmarks (DAVIS, HDTF), BBF achieves lower FVD with competitive FID and LPIPS. On audio-visual synchronized interpolation (HDTF, Hallo3), BBF further surpasses recent audio-driven avatar models on five out of six metrics, including 9.3% FID and 38.8% FVD gains over StableAvatar on Hallo3.

In summary, our contributions are listed as follows:

- To meet the demands of diverse VFI applications, especially those involving fast, nonlinear motion over extended time spans at fine granularity, we optimize the

input conditioning and establish a unified conditioning paradigm to yield a more contextualized, robust, and fine-grained diffusion process.

- We introduce BBF, a context-aware video frame interpolation framework which could be guided by audio/visual semantics. In addition, we propose a decoupled cross-modal fusion mechanism to effectively strengthen the denoising process.
- We design a progressive training paradigm. As training proceeds, we dynamically adjust model weighting, gradually shifting from context-semantic cues to audio-driven cues and from global image content to facial and lip details. Furthermore, extensive ablations validate its effectiveness.
- Compared with state-of-the-art methods in frame interpolation and audio-driven video generation, BBF achieves superior performance on benchmarks featuring fast, non-linear, and long-range fine-grained motion.

2. Related work

Traditionally, VFI task is formulated as an energy minimization problem [2, 5, 19, 20] under brightness constancy and local smoothness assumptions. Recently, most of VFI methods focus on modeling the intermediate optical flow by estimating pixel-wise correspondences from the source to the target frame, followed by forward warping [38] or backward warping [10, 22, 28, 29, 32] to synthesize the target frame. For example, VFIMamba [57] leverages a global receptive field through a state-space formulation to capture motion, while SGM-VFI [30] refines the estimated flow via sparse global matching.

With the advent of large-scale datasets [35–37] and advanced network architectures [14, 21, 47, 48], learning-based methods have made substantial progress. Some approaches [33, 43] apply diffusion models [17, 40, 46] to VFI and report promising results. These diffusion models are specifically designed for flow estimation and trained with ground-truth flow. LDMVFI [43] employs a latent diffusion framework to synthesize the intermediate frame conditioned on given frames. LBBDM [34] uses a continuous Brownian-bridge diffusion process to denoise a latent initialized from random noise toward the target frame. MAD-IF [24] conditions the diffusion process on motion cues to generate the intermediate frame, and Vidim [25] adopts a cascaded diffusion design to produce the target frame. However, despite their advantages, these U-Net-based diffusion models, with convolution backbones, still struggle with accurately capturing large. Accordingly, more recent methods [61] built on a DiT backbone to strengthen temporal attention and guide the synthesis of coherent motion. In addition, several interpolation methods [11, 25, 42, 55], such as Wan 2.1, have begun to exploit text inputs to guide the synthesis of in-between frames. While these approaches

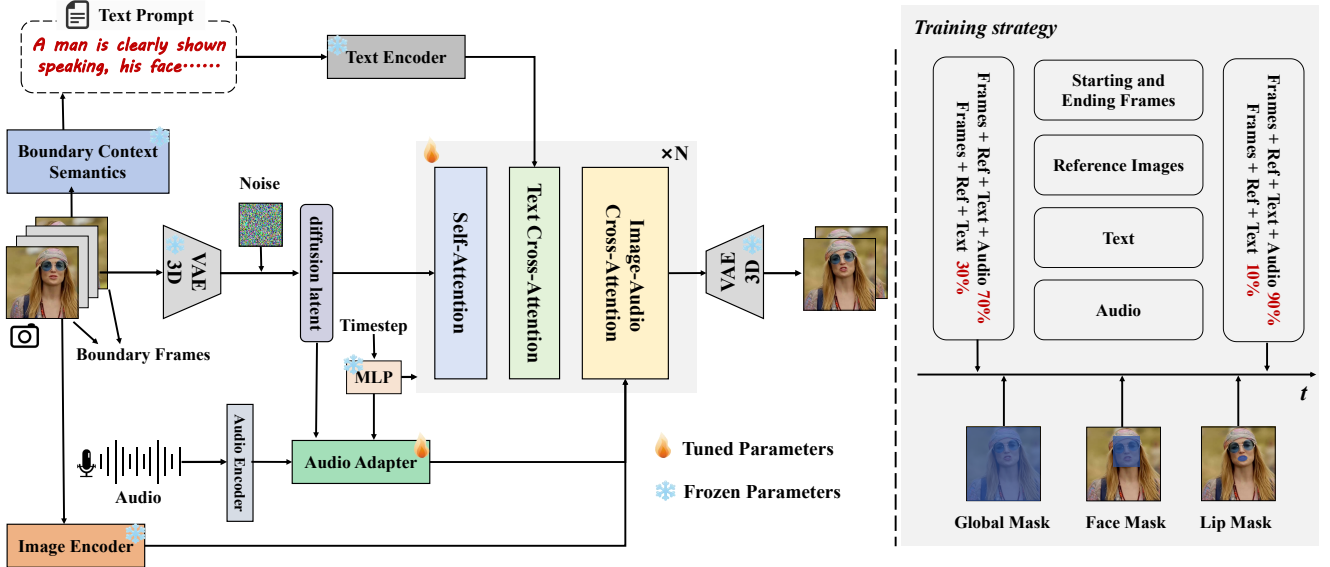


Figure 1. The overall framework of BBF. Our model (left) is trained based on the proposed data processing pipeline (right). Built on a DiT-based backbone, the model introduces a decoupled multimodal fusion mechanism and adopts a progressively aligned training strategy. BBF enables video frame interpolation under various modality combinations.

can perform interpolation between start–end frames over short temporal spans, they do not fully meet the needs of diverse scenarios, particularly those involving fast, non-linear micro-motions over longer windows, such as the audio-visual synchronized interpolation tasks [13, 26]. In particular, talking-head animation [4, 7, 54, 59, 60] is one of the most typical applications of audio–visual driven video generation. In this setting, when local segments of a synthesized video need to be corrected, the corresponding subsequences must be regenerated via video frame interpolation. However, existing interpolation methods are insufficient for such fine-grained, context-dependent corrections and often struggle to produce videos that are both semantically precise and temporally consistent. Inspired by prior work [13, 49], we adopt Wan2.1 [52] as our backbone and introduce targeted modifications to tailor it for audio-visual semantics guided, context-aware video frame interpolation.

3. Method

Our goal is to deliver a more effective and resilient diffusion model in VFI task from the perspective of input condition, model architecture, and training paradigm. To do so, we present the framework BBF where we design a context-aware video frame interpolation framework that could be guided by audio and visual semantics. Figure 1 illustrates the pipeline. In the following sections, we analyze the technical details of how each of the aspects is implemented.

3.1. Input condition

Existing interpolation models typically synthesize the intermediate frame by modeling optical flow. These meth-

ods treat optical flow as a strong supervisory or guiding signal. As a result, the solution space contracts toward low-curvature trajectories consistent with endpoint extrapolation, thereby diminishing the ability of audio and text to drive high-frequency complex motions, such as instantaneous phoneme opening/closure). Accordingly, we provide a theoretical analysis. Let the start/end frames be I_0, I_1 and the endpoint optical flows be $F_{0 \rightarrow 1}$ and $F_{1 \rightarrow 0}$. Classical interpolation forms the in-between frame as a reprojection under extrapolated flows:

$$\hat{I}_\alpha = \mathcal{W}(I_0, \alpha F_{0 \rightarrow 1}) \oplus \mathcal{W}(I_1, (1 - \alpha) F_{1 \rightarrow 0}) \quad (1)$$

where $\alpha \in [0, 1]$ is normalized time; \mathcal{W} denotes backward warping; and \oplus indicates occlusion-aware compositing. In addition, We minimize the reprojection error of \hat{I}_α with a flow-smoothness regularizer:

$$\mathcal{L} = \sum_\alpha \|I_\alpha - \hat{I}_\alpha\|_2^2 + \lambda \sum_x \|\nabla F(x)\|_2^2 \quad (2)$$

On the pixel-trajectory level, denote the position of the same physical point at time t by \mathbf{p}_t . From (1) and (2), one obtains the following trajectory-energy approximation:

$$\mathcal{E} = \sum_t \|\Delta \mathbf{p}_t - \mathbf{v}^*\|_2^2 + \lambda_s \sum_t \|\Delta^2 \mathbf{p}_t\|_2^2, \quad (3)$$

where $\Delta \mathbf{p}_t = \mathbf{p}_{t+1} - \mathbf{p}_t$ denotes per-step velocity, $\Delta^2 \mathbf{p}_t = \mathbf{p}_{t+1} - 2\mathbf{p}_t + \mathbf{p}_{t-1}$ denotes discrete acceleration, and \mathbf{v}^* is the endpoint-consistent target velocity. Additionally, taking the first-order optimality condition of the trajectory energy yields $\Delta^2 \mathbf{p}_t \approx 0$, whose solution is

$$\mathbf{p}_t \approx \mathbf{p}_0 + t \mathbf{v}^*. \quad (4)$$

where t indexes discrete time steps between the endpoints. Equation (4) shows that the trajectory tends to be near constant-velocity, which means low curvature.

Accordingly, strong optical-flow supervision and guidance tends to contract the feasible solution space toward smooth, endpoint-consistent extrapolations, which in turn undermines the model’s capacity to generate context-aware semantics under audio-visual guidance. To mitigate this bias, we prioritize non-visual conditions (audio/text) to drive intermediate-frame synthesis, and design a modality-adaptive conditioning set that admits text, audio, image, and video as interchangeable signals, which enables the model to accommodate diverse interpolation scenarios. Moreover, this design enables the model to inject gated multimodal priors that are semantically and rhythmically informative for different interpolation scenarios preserving consistency with the endpoints.

3.2. Modified Architecture

Illustrated in Figure 1, BBF is based on the commonly used Wan2.1, using DiT as backbone. However, we refine the architecture to integrate start–end video constraints and synchronized audio cues within a unified framework, which can yield fine-grained, audio-driven video dynamics.

Tokenization (1) *For video input.* We firstly employ a pretrained Qwen3-VL-7B to convert the video into descriptive text covering content category, human actions, appearance attributes, and environment. In addition, we take the last frame of the start clip and the first frame of the end clip as reference images. (2) *For text input.* The text sequence is encoded by a standard text encoder into discrete token embeddings, which are fed into each text cross-attention block of the denoising DiT to enhance the interpolated video’s consistency with the surrounding content and context. (3) *For images input.* The reference frames are processed through the diffusion model via two pathways. Firstly, We connect the boundary frames along the temporal axis by inserting zero-padded placeholder frames, and form a fixed-length sequence. This sequence is then transformed into latents by a frozen 3D VAE Encoder. In addition, the start frame is encoded by a CLIP image encoder to obtain an image embedding, which is passed to each image–audio cross-attention block of the denoising DiT to modulate appearance. (4) *For audio input.* We extract the audio embedding a_t utilizing Wav2Vec. The embedding a_t is then passed to an audio adapter that is fine-tuned using the start-end latent difference of the video. The audio adapter jointly models the temporal offset and the audio representation, and aligns the audio features with the primary query tokens, thereby producing a refined embedding \bar{a}_t . Finally, we inject \bar{a}_t into the DiT blocks via cross-attention, guiding the model toward the audio-conditioned generative distribution.

Decoupled cross-modal fusion Our latent tokens interact continuously with the starting and ending frames during compression, building representations with strong temporal alignment. However, U-Net-based diffusion models, with convolution backbones, struggle to capture temporal dynamics. Therefore, BBF adopts a DiT generator as the core synthesis module and processes 3D-VAE latents $\mathbf{Z} \in \mathbb{R}^{T \times H' \times W' \times D}$ as the primary query sequence. For processing the primary query sequence \mathbf{Z} , we propose introduce a video interpolation masking mechanism grounded in pixel-level constraints on the start and end frames. At inference, the model pins the starting and ending frames to the first and last positions along the temporal dimension, with a mask enforcing these positions to remain hard pixel-level conditions throughout computation. Subsequently, the entire sequence is fed once into a 3D-VAE to obtain a temporally ordered latent sequence. On top of this representation, the model applies global attention along the temporal axis, so that at each denoising step every position can directly attend to the starting and ending latents. Importantly, this design ensures that the model is explicitly conditioned on the full start–end constraint at every denoising step, thereby achieving strict alignment of endpoint poses and stably guiding the synthesis of the in-between segment. Beyond the primary query, the model is conditioned via cross-attention on three streams: text embeddings, image embeddings, and audio embeddings, which provide semantic, visual, and temporal cues. We employ a decoupled cross-attention scheme. Firstly, text is injected to establish semantic intent, ensuring consistency with the preceding and following content as well as the scene. Subsequent to the text cross-attention, the reference image and audio are injected through a shared branch to improve visual fidelity and temporal coherence. By coordinating semantic, visual, and temporal interactions at every denoising step, this design leads to improved video interpolation performance.

3.3. Training Paradigm

Progressive alignment To avoid early over-reliance on audio prior to adequate acquisition of the start–end constraints, we employ a staged training paradigm that firstly stabilizes the endpoint constraints and then progressively increases audio conditioning. Concretely, during the early training phase, we randomly mask the audio features with probability 0.3, encouraging the model to focus on textual and visual cues. The setting compels the model to complete interpolation without audio, thereby consolidating start–end consistency and preserving contextual semantics. As training proceeds, we anneal the audio masking rate to 0.1, allowing audio to progressively dominate the generation process, which is significant to ensure high alignment in both appearance and temporal dynamics. Overall, this staged training yields more stable convergence and impor-

tantly improves both interpolation fidelity and audio–visual synchrony.

Region-focused supervision Our model is trained with the reconstruction loss. In addition, we introduce face masks M_{face} and lip masks M_{lip} , extracted from the input video frames using MediaPipe, to enhance modeling of the facial and lip regions. We define a continuous weight map:

$$W = 1 + \lambda_f(s) M_{\text{face}} + \lambda_l(s) M_{\text{lip}}, \quad (5)$$

where $\lambda_f(s), \lambda_l(s) > 0$ are constants, and $\lambda_f(s)$ and $\lambda_l(s)$ are respectively schedulable coefficients used to emphasize facial structure and lip articulation. Furthermore, s denotes the current training step, which optionally normalized as $\tilde{s} = s/S \in [0, 1]$ with S the total number of steps. With the weight map W defined above, we then optimize the following reconstruction objective:

$$\mathcal{L}_{\text{rec}} = \mathbb{E}[\| (z_{\text{gt}} - z_{\theta}) \odot W \|_2^2], \quad (6)$$

where z_{gt} and z_{θ} denote the target and predicted latents at the same time step; $(z_{\text{gt}} - z_{\theta})$ denote the element-wise residual. Additionally, \odot denotes element-wise multiplication, define a continuous weight map, and $\mathbb{E}[\cdot]$ averages over batches, time indices, and spatial locations. In general, the weights $\lambda_f(s), \lambda_l(s)$ evolve dynamically with progress during training. In the initial phase, the model emphasizes the global spatial layout, encouraging it to first internalize the global motion implied by the target keyframes. In the later phase, the emphasis shifts toward the lip mask, directing more attention to audio-synchronization details. This progressive focusing strategy guides the model to perform coarse interpolation first, followed by refinement of facial and articulatory motions.

4. Experiments

4.1. Implementation Details

Dataset. Our training dataset is Celebv-HQ [63] containing 35,666 celebrity face video clips at a minimum resolution of 512×512, where each clip lasts 3-20 seconds. To evaluate the performance of the model in fast, non-linear, fine-grained motion over a longer time window, we compare against strong baselines from both video frame interpolation and audio-synchronized talking-head generation. Accordingly, we conduct evaluations on DAVIS [41], HDTF [60] and Hallo3 [9]. DAVIS is a widely used benchmark for large motions, containing 2,849 triplets at a resolution of 480×854. HDTF is a high-resolution, in-the-wild talking-face dataset consisting of hundreds of frontal videos captured at 720p/1080p, widely used for audio-driven talking-head generation and evaluation. Additionally, Hallo3, which is a recent CVPR ’25 benchmark, fea-

tures over 70 hours of talk footage and approximately 50 hours of dynamic portrait editing.

Hyperparameters. Our DiT uses pre-trained weights of Wan2.1-I2V 1.3B [31, 52] as the backbone. We fine-tune BBF on four A100-80G GPUs with a per-GPU batch size of 8 and no data augmentation beyond the normalization already present in the dataset pipeline. Following the training script, we use AdamW with $\beta_1 = 0.9, \beta_2 = 0.999$ and set learning rate to 2×10^{-5} . We train the model for 2,000 steps and save checkpoints every 100 steps. Additionally, VAE, CLIP, T5, and Wav2Vec [1] remain frozen, while only the DiT attention stacks and the audio adapter are updated.

Evaluation metrics. We evaluate BBF against two groups of baselines: (1) general-purpose video VFI methods and (2) audio-driven talking-head methods. For the video interpolation models, we use FID [16] and FVD [50] to evaluate the quality of the synthesized images and videos. Additionally, we introduce LPIPS [58] to quantify the perceptual distance between generated frames and ground-truth frames. For talking-head animation, in addition to using FID, FVD, and LPIPS as evaluation metrics, SyncD [8] is utilized to assess the synchronization of lips with audio. Moreover, we also introduce PSNR [18] to measure the pixel fidelity of the generated images and SSIM [53] to evaluate the structural similarity between the generated images and the real images.

4.2. Comparison with State-of-the-Art Methods

To comprehensively evaluate the effectiveness of our model on the video frame interpolation task, we compare against two classes of baselines. Firstly, we benchmark BBF against general-purpose VFI methods, including approaches conditioned on optical flow or on text. Secondly, to further examine performance on audio-synchronized interpolation tasks that are fast, non-linear, we adopt the canonical audio-synchronized talking-head generation setting as a counterpart task and compare with representative methods.

Quantitative results. On the basic interpolation benchmark, we compare quantitatively it with both traditional optical flow–based methods and recent diffusion-based approaches on DAVIS and HDTF. Specifically, we include TRF [11], LBBDM [34], AMT [29], VFIMamba [57], EDEN [61], DynamiCrafter [55] and Wan2.1 [52] for comparison. To ensure a fair comparison, we do not introduce any additional conditioning signals to boost our model’s performance. The results are shown in Table 1. For DAVIS, it is obvious that BBF overall outperform all other methods, achieving a FID of 262.30, a FVD of 1034.41 and an LPIPS

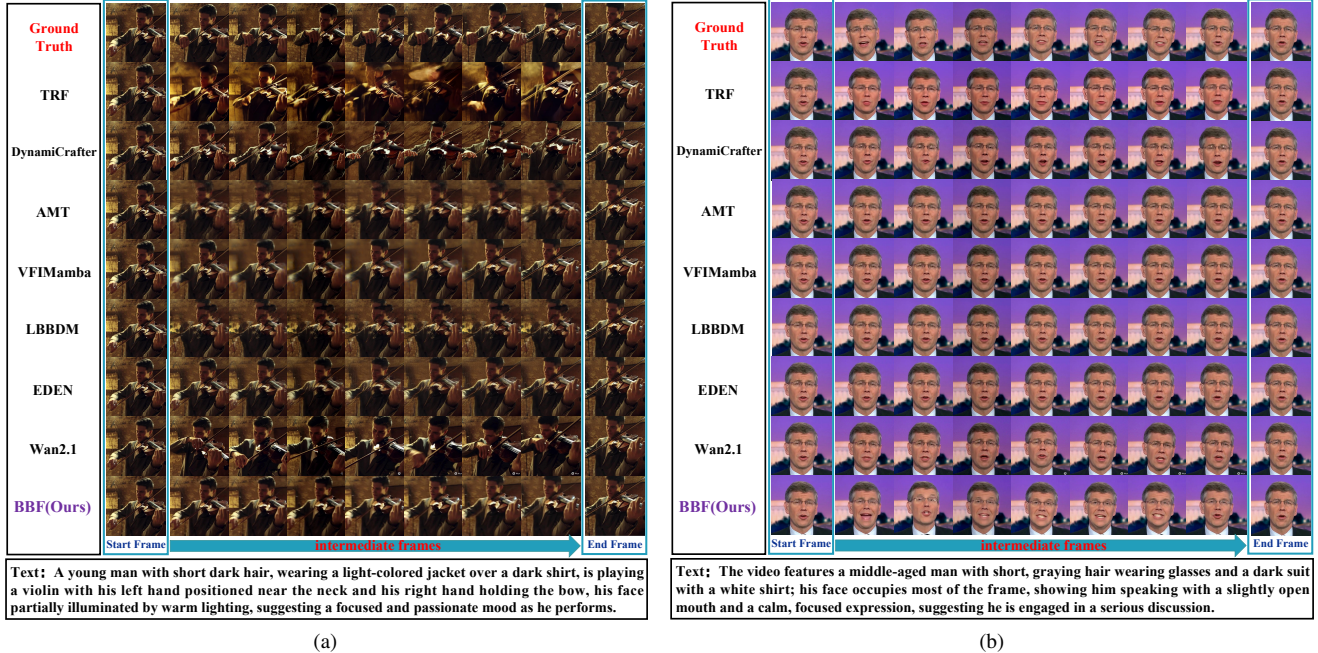


Figure 2. **Qualitative comparison with video frame interpolation methods on different scenarios.** (a) Generic scene from DAVIS dataset showing a violin performance with large motion. (b) Talking face scene from HDTF dataset demonstrating audio-synchronized interpolation. Our method achieves better motion continuity, identity preservation, and temporal consistency compared to VFI methods.

of 0.54. For HDTF, BBF also achieves the best overall results on this more dynamic, fine-grained dataset, with a FID of 10.50, a FVD of 174.24 and an LPIPS of 0.12. Consequently, BBF attains performance comparable to prior VFI models and even surpasses some methods that only accept text and boundary frames inputs.

Table 1. **Quantitative comparison with video frame interpolation (VFI) methods on DAVIS and HDTF datasets.**

Model	DAVIS			HDTF		
	FID	FVD	LPIPS	FID	FVD	LPIPS
TRF	303.58	2976.62	0.58	13.82	450.10	0.15
EDEN	397.26	1963.53	0.58	9.23	859.73	0.12
AMT	397.33	<u>1869.40</u>	0.65	10.07	954.95	0.12
VFIMamba	431.94	2325.39	0.65	9.91	752.59	0.12
LBBDM	398.62	2085.42	0.60	11.07	919.46	0.12
DynamiCrafter	456.63	2624.00	0.93	13.49	<u>181.53</u>	0.15
Wan2.1	<u>292.35</u>	2427.15	0.49	<u>9.43</u>	237.02	0.14
BBF (Ours)	262.30	1034.41	<u>0.54</u>	10.50	174.24	0.12

For talking-head animation, we compare with current audio-driven avatar video generation models, including GAN-based models (SadTalker [59]) and diffusion-based models (SD-based: Aniporrait [54], EchoMimic [7]; SVD-based: Sonic [26]; Wan-14B-based: OminiAvatar [13]; Wan-1.3B-based: Stableavatar [49]). Based on prior studies, we conduct quantitative comparisons with the above

competitors on HDTF and Hallo3. Notably, because some previous works did not release their test datasets, we randomly select and crop 20 video segments (3-5 seconds) from each of HDTF and Hallo3 to ensure a fair comparison. The results are shown in Table 2. On the two test sets, except that the Sync-D metric is slightly worse than the current best score, our model achieves the leading scores on the other five metrics, which means that our model surpasses them in terms of face quality, video fidelity, and lip synchronization. Specifically, on Hallo3, BBF exceeds the strongest competitor Stableavatar based on Wan2.1-1.3B by 9.3% on FID and 38.8% on FVD. This further indicates that our model can better meet the needs of the video frame interpolation task guided by audio-visual semantics.

Qualitative Results. Figures 2 and 3 present intuitive comparisons between BBF and previous methods in different scenarios. Based on the DAVIS dataset, Figure 2(a) presents the performance of each method in a generic scene under the same input start/end frames and text conditions. In the scene of playing the violin, the performer’s hands and the instrument undergo large motions. Optical-flow-based interpolation methods (LBBDM, AMT, VFIMamba) often produce tearing or ghosting artifacts around the fingers and facial details, whereas diffusion-based methods (BBF, EDEN, Wan2.1), except for TRF and DynamiCrafter, better preserve the performer’s identity consistency and the temporal continuity of motion. Based on the HDTF talking-

Table 2. **Quantitative comparison with state-of-the-art audio-driven talking head methods on HDTF and Hallo3 datasets.** Lower is better for FID/FVD/LPIPS/Sync-D (\downarrow); higher is better for PSNR/SSIM (\uparrow). Bold indicates the best results (ties bolded); underline indicates second best.

Model	HDTF						Hallo3					
	FID \downarrow	FVD \downarrow	LPIPS \downarrow	PSNR \uparrow	SSIM \uparrow	Sync-D \downarrow	FID \downarrow	FVD \downarrow	LPIPS \downarrow	PSNR \uparrow	SSIM \uparrow	Sync-D \downarrow
SadTalker	51.60	405.91	0.41	15.33	0.62	1.34	113.34	2890.96	0.64	9.66	0.36	0.84
Aniportrait	46.31	480.04	0.31	16.49	0.61	<u>1.36</u>	41.40	1338.44	0.54	10.39	<u>0.42</u>	1.38
EchoMimic	53.27	484.89	0.43	14.58	0.59	3.76	115.57	2233.90	0.68	9.59	0.36	1.56
Sonic	45.02	366.21	0.26	18.05	0.64	4.69	38.19	1710.88	0.52	10.48	0.39	4.60
OminiAvatar	35.34	441.10	0.23	19.54	<u>0.69</u>	7.64	46.58	1976.81	0.52	<u>10.65</u>	<u>0.42</u>	7.28
StableAvatar	<u>31.61</u>	<u>318.12</u>	<u>0.21</u>	<u>19.68</u>	0.68	2.79	<u>35.21</u>	<u>1262.70</u>	0.54	10.54	<u>0.42</u>	4.50
BBF (Ours)	25.01	297.70	0.18	20.44	0.72	1.90	31.95	773.00	0.52	10.86	0.44	1.42

face dataset, Fig. 2(b) visually demonstrates the superiority of BBF in audio-synchronized interpolation tasks. When facing fast, non-linear, fine-grained motion, other methods frequently generate ghosting artifacts around the mouth and glasses in intermediate frames. Additionally, the lip movements are overly smoothed, thereby failing to achieve accurate audio-visual alignment. In contrast, the intermediate frames generated by BBF exhibit higher visual fidelity and stronger identity consistency. Furthermore, the lip shapes and facial motions evolve continuously over time, remaining highly consistent with the speech content. This fully indicates that BBF can stably perform context-aware modeling guided by audio-visual semantics, while maintaining both global structure and local details during generation.

To further demonstrate the irreplaceability of BBF in audio-visual synchronized interpolation tasks, Fig. 3 shows qualitative visualization results of each method in the talking-head animation scenario. Existing baseline methods often suffer from overly rigid head poses, blurred teeth and lip contours, and identity drift in speech segments with rapid phoneme transitions. In contrast, our model produces sharper facial details, more natural and smooth face motions. Additionally, the lip movements follow the audio rhythm more accurately. More importantly, given the requirements of interpolation scenarios, existing methods fail to ensure a natural transition between the generated clip and the subsequent content in the original video. This further shows that, under boundary-frame constraints, BBF can handle different scenarios, including generic VFI and audio-driven, context-aware interpolation.

Human Evaluation. We conducted a human evaluation to assess the perceptual quality of generated talking head videos. Thirty participants rated seven state-of-the-art methods across three dimensions: lip synchronization, body movement realism, and temporal coherence, using a 5-point Likert scale. Given our VFI-enhanced approach’s focus on temporal frame manipulation, these dimensions specifically

evaluate audio-visual alignment preservation during interpolation, motion naturalness, and smoothness across interpolated frames. To ensure fair comparison, we evaluated only video segments requiring interpolation or editing, as baseline methods do not support contextual inputs. Videos were presented in random order to avoid bias. As shown in Fig. 4, our method achieved the highest scores across all dimensions (4.23 ± 0.58 , 4.15 ± 0.53 , 4.31 ± 0.46), significantly outperforming other methods, with low variance indicating robust and consistent performance. Statistical analysis confirmed significant improvements ($p < 0.01$ for lip synchronization, $p < 0.05$ for others).

4.3. Ablation Study

Input condition. To isolate the contribution of each input condition, we conduct an ablation with three variants: (1) text only; (2) audio only; and (3) text + audio. Results are reported in Table 3. Text-only obtains the best FID and PSNR/SSIM but the worst Sync-D, showing that text alone cannot ensure precise audio-visual alignment. Audio-only improves synchronization at the cost of visual fidelity, while combining text and audio yields the best Sync-D and FVD with competitive FID/PSNR/SSIM, confirming the benefit of multi-channel conditioning in BBF.

Table 3. Ablation study of input modalities on HDTF.

Conditions	HDTF					
	FID \downarrow	FVD \downarrow	LPIPS \downarrow	PSNR \uparrow	SSIM \uparrow	Sync-D \downarrow
Text	29.98	826.60	0.18	21.70	0.75	1.09
Audio	36.52	427.43	0.19	20.82	0.73	0.90
Text & Audio	37.16	343.02	0.20	20.36	0.71	0.73

Table 4. Ablation study of training paradigm on HDTF

Audio mask	HDTF					
	FID \downarrow	FVD \downarrow	LPIPS \downarrow	PSNR \uparrow	SSIM \uparrow	Sync-D \downarrow
30% (fixed)	10.74	174.24	0.15	22.11	0.78	1.39
10% (fixed)	12.45	246.10	0.16	21.76	0.77	2.04
30% \rightarrow 10%	10.50	187.02	0.14	22.41	0.78	0.66



Figure 3. **Qualitative evaluation against audio-driven talking head generation methods on HDTF.** Our method produces sharper facial details, smoother motion, and better audio-lip synchronization while maintaining natural transitions with boundary frames.

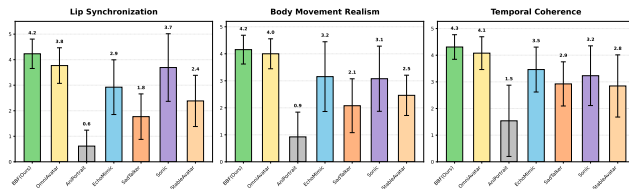


Figure 4. **Human evaluation results among our proposed BBF and other SoTA methods.**

Training Paradigm. To validate the necessity of the staged training paradigm, we conducted an ablation study on training paradigm using the HDTF dataset. Based on different training paradigms, we train the model for 200 steps under three variants to compare performance: (1) randomly mask audio features with probability 0.3 throughout; (2) randomly mask audio features with probability 0.1 throughout; (3) a staged paradigm that masks at 30% for the first 100 steps and reduces to 10% for the last 100 steps. The results are detailed in Table 4. Under identical text, audio, and boundary-frame inputs, the staged training paradigm achieves the best performance on five of six metrics, indicating more stable convergence with improved visual fidelity and temporal consistency.

5. Applications

BBF can be easily adapted to support additional applications. **i). Correction of talking-head animation.** In speech-driven scenarios, local errors in a video are fixed by

resynthesizing the corresponding segments via frame interpolation. BBF instead leverages the segment’s audio to regenerate clips that remain consistent with the surrounding context. **ii). Background-audio-guided interpolation.** With light additional training, our framework also supports interpolation driven by background audio. We condition on boundary frames and text, replacing speech with background audio during training so the model generates interpolated clips consistent with the acoustic context.

6. Conclusion

In this paper, we introduce BBF, a context-aware, audio-visual guided framework for video interpolation that targets diverse real-world scenarios, particularly those with fast, non-linear, and long-range fine-grained motions. Our framework can adaptively accept multiple modal conditioning signals to provide a more contextualized and resilient diffusion process. To achieve more effective multimodal fusion, we adopt a decoupled cross-modal fusion mechanism and introduce an audio adapter with temporal attentiveness to ensure temporal consistency in the generated videos. By embedding the starting and ending frames differencing into the training paradigm, BBF more effectively balances global structure and local details in synthesis. Extensive experiments demonstrated that BBF achieves state-of-the-art performance across a variety of benchmarks, validating its versatility in diverse application scenarios. Future work will further enhance the model’s modeling of contextual emotions and extend it toward robust generalization in multilingual scenarios.

References

- [1] Alexei Baevski, Yuhao Zhou, Abdelrahman Mohamed, and Michael Auli. wav2vec 2.0: A framework for self-supervised learning of speech representations. *Advances in neural information processing systems*, 33:12449–12460, 2020. 5
- [2] Michael J Black and Padmanabhan Anandan. A framework for the robust estimation of optical flow. In *1993 (4th) International Conference on Computer Vision*, pages 231–236. IEEE, 1993. 2
- [3] Tim Brooks and Jonathan T Barron. Learning to synthesize motion blur. In *Proceedings of the IEEE/CVF Conference on Computer Vision and Pattern Recognition*, pages 6840–6848, 2019. 1
- [4] Liyang Chen, Tianxiang Ma, Jiawei Liu, Bingchuan Li, Zhuowei Chen, Lijie Liu, Xu He, Gen Li, Qian He, and Zhiyong Wu. Humo: Human-centric video generation via collaborative multi-modal conditioning. *arXiv preprint arXiv:2509.08519*, 2025. 3
- [5] Qifeng Chen and Vladlen Koltun. Full flow: Optical flow estimation by global optimization over regular grids. In *Proceedings of the IEEE conference on computer vision and pattern recognition*, pages 4706–4714, 2016. 2
- [6] Zeyuan Chen, Yinbo Chen, Jingwen Liu, Xingqian Xu, Vidit Goel, Zhangyang Wang, Humphrey Shi, and Xiaolong Wang. Videoir: Learning video implicit neural representation for continuous space-time super-resolution. In *Proceedings of the IEEE/CVF Conference on Computer Vision and Pattern Recognition*, pages 2047–2057, 2022. 1
- [7] Zhiyuan Chen, Jiajiong Cao, Zhiquan Chen, Yuming Li, and Chenguang Ma. Echomimic: Lifelike audio-driven portrait animations through editable landmark conditions. In *Proceedings of the AAAI Conference on Artificial Intelligence*, pages 2403–2410, 2025. 3, 6
- [8] Joon Son Chung and Andrew Zisserman. Out of time: automated lip sync in the wild. In *Asian conference on computer vision*, pages 251–263. Springer, 2016. 5
- [9] Jiahao Cui, Hui Li, Yun Zhan, Hanlin Shang, Kaihui Cheng, Yuqi Ma, Shan Mu, Hang Zhou, Jingdong Wang, and Siyu Zhu. Hallo3: Highly dynamic and realistic portrait image animation with video diffusion transformer. In *Proceedings of the Computer Vision and Pattern Recognition Conference*, pages 21086–21095, 2025. 5
- [10] Duolikun Danier, Fan Zhang, and David Bull. St-mfnet: A spatio-temporal multi-flow network for frame interpolation. In *Proceedings of the IEEE/CVF Conference on Computer Vision and Pattern Recognition*, pages 3521–3531, 2022. 2
- [11] Haiwen Feng, Zheng Ding, Zhihao Xia, Simon Niklaus, Victoria Abrevaya, Michael J Black, and Xuaner Zhang. Explorative inbetweening of time and space. In *European Conference on Computer Vision*, pages 378–395. Springer, 2024. 1, 2, 5
- [12] John Flynn, Ivan Neulander, James Philbin, and Noah Snavely. Deepstereo: Learning to predict new views from the world’s imagery. In *Proceedings of the IEEE conference on computer vision and pattern recognition*, pages 5515–5524, 2016. 1
- [13] Qijun Gan, Ruizi Yang, Jianke Zhu, Shaofei Xue, and Steven Hoi. Omniavatar: Efficient audio-driven avatar video generation with adaptive body animation. *arXiv preprint arXiv:2506.18866*, 2025. 3, 6
- [14] Yang Hai, Rui Song, Jiaojiao Li, and Yinlin Hu. Shape-constraint recurrent flow for 6d object pose estimation. In *Proceedings of the IEEE/CVF conference on computer vision and pattern recognition*, pages 4831–4840, 2023. 2
- [15] Yang Hai, Guo Wang, Tan Su, Wenjie Jiang, and Yinlin Hu. Hierarchical flow diffusion for efficient frame interpolation. In *Proceedings of the Computer Vision and Pattern Recognition Conference*, pages 22943–22952, 2025. 1
- [16] Martin Heusel, Hubert Ramsauer, Thomas Unterthiner, Bernhard Nessler, and Sepp Hochreiter. Gans trained by a two time-scale update rule converge to a local nash equilibrium. *Advances in neural information processing systems*, 30, 2017. 5
- [17] Jonathan Ho, Ajay Jain, and Pieter Abbeel. Denoising diffusion probabilistic models. *Advances in neural information processing systems*, 33:6840–6851, 2020. 2
- [18] Alain Hore and Djemel Ziou. Image quality metrics: Psnr vs. ssim. In *2010 20th international conference on pattern recognition*, pages 2366–2369. IEEE, 2010. 5
- [19] Yinlin Hu, Rui Song, and Yunsong Li. Efficient coarse-to-fine patchmatch for large displacement optical flow. In *Proceedings of the IEEE Conference on Computer Vision and Pattern Recognition*, pages 5704–5712, 2016. 2
- [20] Yinlin Hu, Yunsong Li, and Rui Song. Robust interpolation of correspondences for large displacement optical flow. In *Proceedings of the IEEE conference on computer vision and pattern recognition*, pages 481–489, 2017. 2
- [21] Zhaoyang Huang, Xiaoyu Shi, Chao Zhang, Qiang Wang, Ka Chun Cheung, Hongwei Qin, Jifeng Dai, and Hongsheng Li. Flowformer: A transformer architecture for optical flow. In *European conference on computer vision*, pages 668–685. Springer, 2022. 2
- [22] Zhewei Huang, Tianyuan Zhang, Wen Heng, Boxin Shi, and Shuchang Zhou. Real-time intermediate flow estimation for video frame interpolation. In *European Conference on Computer Vision*, pages 624–642. Springer, 2022. 1, 2
- [23] Zhewei Huang, Ailin Huang, Xiaotao Hu, Chen Hu, Jun Xu, and Shuchang Zhou. Scale-adaptive feature aggregation for efficient space-time video super-resolution. In *Proceedings of the IEEE/CVF winter conference on applications of computer vision*, pages 4228–4239, 2024. 1
- [24] Zhilin Huang, Yijie Yu, Ling Yang, Chujun Qin, Bing Zheng, Xiawu Zheng, Zikun Zhou, Yaowei Wang, and Wenming Yang. Motion-aware latent diffusion models for video frame interpolation. In *Proceedings of the 32nd ACM International Conference on Multimedia*, pages 1043–1052, 2024. 1, 2
- [25] Siddhant Jain, Daniel Watson, Eric Tabellion, Ben Poole, Janne Kontkanen, et al. Video interpolation with diffusion models. In *Proceedings of the IEEE/CVF Conference on Computer Vision and Pattern Recognition*, pages 7341–7351, 2024. 1, 2

- [26] Xiaozhong Ji, Xiaobin Hu, Zhihong Xu, Junwei Zhu, Chuming Lin, Qingdong He, Jiangning Zhang, Donghao Luo, Yi Chen, Qin Lin, et al. Sonic: Shifting focus to global audio perception in portrait animation. In *Proceedings of the Computer Vision and Pattern Recognition Conference*, pages 193–203, 2025. 3, 6
- [27] Huaizu Jiang, Deqing Sun, Varun Jampani, Ming-Hsuan Yang, Erik Learned-Miller, and Jan Kautz. Super slomo: High quality estimation of multiple intermediate frames for video interpolation. In *Proceedings of the IEEE conference on computer vision and pattern recognition*, pages 9000–9008, 2018. 1
- [28] Lingtong Kong, Boyuan Jiang, Donghao Luo, Wenqing Chu, Xiaoming Huang, Ying Tai, Chengjie Wang, and Jie Yang. Ifrnet: Intermediate feature refine network for efficient frame interpolation. In *Proceedings of the IEEE/CVF Conference on Computer Vision and Pattern Recognition*, pages 1969–1978, 2022. 1, 2
- [29] Zhen Li, Zuo-Liang Zhu, Ling-Hao Han, Qibin Hou, Chun-Le Guo, and Ming-Ming Cheng. Amt: All-pairs multi-field transforms for efficient frame interpolation. In *Proceedings of the IEEE/CVF Conference on Computer Vision and Pattern Recognition*, pages 9801–9810, 2023. 2, 5
- [30] Chunxu Liu, Guozhen Zhang, Rui Zhao, and Limin Wang. Sparse global matching for video frame interpolation with large motion. In *Proceedings of the IEEE/CVF conference on computer vision and pattern recognition*, pages 19125–19134, 2024. 1, 2
- [31] Lijie Liu, Tianxiang Ma, Bingchuan Li, Zhuowei Chen, Jiawei Liu, Gen Li, Siyu Zhou, Qian He, and Xinglong Wu. Phantom: Subject-consistent video generation via cross-modal alignment. *arXiv preprint arXiv:2502.11079*, 2025. 5
- [32] Liying Lu, Ruizheng Wu, Huaijia Lin, Jiangbo Lu, and Jiaya Jia. Video frame interpolation with transformer. In *Proceedings of the IEEE/CVF Conference on Computer Vision and Pattern Recognition*, pages 3532–3542, 2022. 2
- [33] Ao Luo, Xin Li, Fan Yang, Jiangyu Liu, Haoqiang Fan, and Shuaicheng Liu. Flowdiffuser: Advancing optical flow estimation with diffusion models. In *Proceedings of the IEEE/CVF Conference on Computer Vision and Pattern Recognition*, pages 19167–19176, 2024. 2
- [34] Zonglin Lyu, Ming Li, Jianbo Jiao, and Chen Chen. Frame interpolation with consecutive brownian bridge diffusion. In *Proceedings of the 32nd ACM International Conference on Multimedia*, pages 3449–3458, 2024. 1, 2, 5
- [35] Nikolaus Mayer, Eddy Ilg, Philip Hausser, Philipp Fischer, Daniel Cremers, Alexey Dosovitskiy, and Thomas Brox. A large dataset to train convolutional networks for disparity, optical flow, and scene flow estimation. In *Proceedings of the IEEE conference on computer vision and pattern recognition*, pages 4040–4048, 2016. 2
- [36] Lukas Mehl, Jenny Schmalfluss, Azin Jahedi, Yaroslava Nalivayko, and Andrés Bruhn. Spring: A high-resolution high-detail dataset and benchmark for scene flow, optical flow and stereo. In *Proceedings of the IEEE/CVF Conference on Computer Vision and Pattern Recognition*, pages 4981–4991, 2023.
- [37] Jisu Nam, Gyuseong Lee, Sunwoo Kim, Hyeonsu Kim, Hyoungwon Cho, Seyeon Kim, and Seungryong Kim. Diffusion model for dense matching. *arXiv preprint arXiv:2305.19094*, 2023. 2
- [38] Simon Niklaus and Feng Liu. Softmax splatting for video frame interpolation. In *Proceedings of the IEEE/CVF conference on computer vision and pattern recognition*, pages 5437–5446, 2020. 2
- [39] Junheum Park, Jintae Kim, and Chang-Su Kim. Biformer: Learning bilateral motion estimation via bilateral transformer for 4k video frame interpolation. In *Proceedings of the IEEE/CVF Conference on Computer Vision and Pattern Recognition*, pages 1568–1577, 2023. 1
- [40] William Peebles and Saining Xie. Scalable diffusion models with transformers. In *Proceedings of the IEEE/CVF international conference on computer vision*, pages 4195–4205, 2023. 1, 2
- [41] Jordi Pont-Tuset, Federico Perazzi, Sergi Caelles, Pablo Arbeláez, Alex Sorkine-Hornung, and Luc Van Gool. The 2017 davis challenge on video object segmentation. *arXiv preprint arXiv:1704.00675*, 2017. 5
- [42] Fitsum A Reda, Deqing Sun, Aysegül Dundar, Mohammad Shoyebi, Guilin Liu, Kevin J Shih, Andrew Tao, Jan Kautz, and Bryan Catanzaro. Unsupervised video interpolation using cycle consistency. In *Proceedings of the IEEE/CVF international conference on computer vision*, pages 892–900, 2019. 2
- [43] Saurabh Saxena, Charles Herrmann, Junhwa Hur, Abhishek Kar, Mohammad Norouzi, Deqing Sun, and David J Fleet. The surprising effectiveness of diffusion models for optical flow and monocular depth estimation. *Advances in Neural Information Processing Systems*, 36:39443–39469, 2023. 2
- [44] Zhihao Shi, Xiangyu Xu, Xiaohong Liu, Jun Chen, and Ming-Hsuan Yang. Video frame interpolation transformer. In *Proceedings of the IEEE/CVF Conference on Computer Vision and Pattern Recognition*, pages 17482–17491, 2022. 1
- [45] Li Siyao, Shiyu Zhao, Weijiang Yu, Wenxiu Sun, Dimitris Metaxas, Chen Change Loy, and Ziwei Liu. Deep animation video interpolation in the wild. In *Proceedings of the IEEE/CVF conference on computer vision and pattern recognition*, pages 6587–6595, 2021. 1
- [46] Jascha Sohl-Dickstein, Eric Weiss, Niru Maheswaranathan, and Surya Ganguli. Deep unsupervised learning using nonequilibrium thermodynamics. In *International conference on machine learning*, pages 2256–2265. pmlr, 2015. 2
- [47] Deqing Sun, Xiaodong Yang, Ming-Yu Liu, and Jan Kautz. Pwc-net: Cnns for optical flow using pyramid, warping, and cost volume. In *Proceedings of the IEEE conference on computer vision and pattern recognition*, pages 8934–8943, 2018. 2
- [48] Zachary Teed and Jia Deng. Raft: Recurrent all-pairs field transforms for optical flow. In *European conference on computer vision*, pages 402–419. Springer, 2020. 2
- [49] Shuyuan Tu, Yueming Pan, Yinming Huang, Xintong Han, Zhen Xing, Qi Dai, Chong Luo, Zuxuan Wu, and Yu-Gang Jiang. Stableavatar: Infinite-length audio-driven avatar video generation. *arXiv preprint arXiv:2508.08248*, 2025. 3, 6

- [50] Thomas Unterthiner, Sjoerd Van Steenkiste, Karol Kurach, Raphael Marinier, Marcin Michalski, and Sylvain Gelly. Towards accurate generative models of video: A new metric & challenges. *arXiv preprint arXiv:1812.01717*, 2018. 5
- [51] Vikram Voleti, Alexia Jolicoeur-Martineau, and Chris Pal. Mcvd-masked conditional video diffusion for prediction, generation, and interpolation. *Advances in neural information processing systems*, 35:23371–23385, 2022. 1
- [52] Team Wan, Ang Wang, Baole Ai, Bin Wen, Chaojie Mao, Chen-Wei Xie, Di Chen, Feiwei Yu, Haiming Zhao, Jianxiao Yang, et al. Wan: Open and advanced large-scale video generative models. *arXiv preprint arXiv:2503.20314*, 2025. 1, 3, 5
- [53] Zhou Wang, Alan C Bovik, Hamid R Sheikh, and Eero P Simoncelli. Image quality assessment: from error visibility to structural similarity. *IEEE transactions on image processing*, 13(4):600–612, 2004. 5
- [54] Huawei Wei, Zejun Yang, and Zhisheng Wang. Aniportrait: Audio-driven synthesis of photorealistic portrait animation. *arXiv preprint arXiv:2403.17694*, 2024. 3, 6
- [55] Jinbo Xing, Menghan Xia, Yong Zhang, Haoxin Chen, Wangbo Yu, Hanyuan Liu, Gongye Liu, Xintao Wang, Ying Shan, and Tien-Tsin Wong. Dynamicrafter: Animating open-domain images with video diffusion priors. In *European Conference on Computer Vision*, pages 399–417. Springer, 2024. 1, 2, 5
- [56] Guozhen Zhang, Yuhan Zhu, Haonan Wang, Youxin Chen, Gangshan Wu, and Limin Wang. Extracting motion and appearance via inter-frame attention for efficient video frame interpolation. In *Proceedings of the IEEE/CVF Conference on Computer Vision and Pattern Recognition*, pages 5682–5692, 2023. 1
- [57] Guozhen Zhang, Chuxnu Liu, Yutao Cui, Xiaotong Zhao, Kai Ma, and Limin Wang. Vfimamba: Video frame interpolation with state space models. *Advances in Neural Information Processing Systems*, 37:107225–107248, 2024. 1, 2, 5
- [58] Richard Zhang, Phillip Isola, Alexei A Efros, Eli Shechtman, and Oliver Wang. The unreasonable effectiveness of deep features as a perceptual metric. In *Proceedings of the IEEE conference on computer vision and pattern recognition*, pages 586–595, 2018. 5
- [59] Wenxuan Zhang, Xiaodong Cun, Xuan Wang, Yong Zhang, Xi Shen, Yu Guo, Ying Shan, and Fei Wang. Sadtalker: Learning realistic 3d motion coefficients for stylized audio-driven single image talking face animation. In *Proceedings of the IEEE/CVF conference on computer vision and pattern recognition*, pages 8652–8661, 2023. 3, 6
- [60] Zhimeng Zhang, Lincheng Li, Yu Ding, and Changjie Fan. Flow-guided one-shot talking face generation with a high-resolution audio-visual dataset. In *Proceedings of the IEEE/CVF conference on computer vision and pattern recognition*, pages 3661–3670, 2021. 3, 5
- [61] Zihao Zhang, Haoran Chen, Haoyu Zhao, Guansong Lu, Yanwei Fu, Hang Xu, and Zuxuan Wu. Eden: Enhanced diffusion for high-quality large-motion video frame interpolation. In *Proceedings of the Computer Vision and Pattern Recognition Conference*, pages 2105–2115, 2025. 1, 2, 5
- [62] Zhihang Zhong, Mingdeng Cao, Xiang Ji, Yinqiang Zheng, and Imari Sato. Blur interpolation transformer for real-world motion from blur. In *Proceedings of the IEEE/CVF Conference on Computer Vision and Pattern Recognition*, pages 5713–5723, 2023. 1
- [63] Hao Zhu, Wayne Wu, Wentao Zhu, Liming Jiang, Siwei Tang, Li Zhang, Ziwei Liu, and Chen Change Loy. Celebv-hq: A large-scale video facial attributes dataset. In *European conference on computer vision*, pages 650–667. Springer, 2022. 5